



HAL
open science

Extension of NXFEM to nonconforming finite elements

Daniela Capatina, H El-Otmany, Didier Graebling, R Luce

► **To cite this version:**

Daniela Capatina, H El-Otmany, Didier Graebling, R Luce. Extension of NXFEM to nonconforming finite elements. *Mathematics and Computers in Simulation*, 2017, 137, pp.226 - 245. 10.1016/j.matcom.2016.12.009 . hal-03482594

HAL Id: hal-03482594

<https://hal.science/hal-03482594>

Submitted on 5 Jan 2022

HAL is a multi-disciplinary open access archive for the deposit and dissemination of scientific research documents, whether they are published or not. The documents may come from teaching and research institutions in France or abroad, or from public or private research centers.

L'archive ouverte pluridisciplinaire **HAL**, est destinée au dépôt et à la diffusion de documents scientifiques de niveau recherche, publiés ou non, émanant des établissements d'enseignement et de recherche français ou étrangers, des laboratoires publics ou privés.

Extension of NXFEM to nonconforming finite elements

D. Capatina^{a,*}, H. El-Otmany^a, D. Graebling^b, R. Luce^a

^aUniversity of Pau, LMAP, Av. de l'Université, 64000 Pau, France

^bUniversity of Pau, IPREM, 2 Av. Angot, 64000 Pau, France

Abstract

In this paper, we consider triangular nonconforming finite element approximations of an interface elliptic problem. We propose two extensions of the conforming Nitsche's extended finite element method to the nonconforming case. The first one is obtained by adding stabilisation terms on the cut edges, and the second one by modifying the Crouzeix-Raviart basis functions on the cut cells. Both discrete problems are uniformly stable and yield optimal *a priori* error estimates, uniformly with respect to the diffusion parameters. Moreover, we show that they exhibit the same robustness with respect to the position of the interface as the classical conforming method. We then validate these results numerically. Finally, we propose a nonconforming approximation of the interface Stokes problem based on the modified Crouzeix-Raviart elements and we illustrate it numerically.

Keywords: interface, NXFEM, nonconforming finite elements, robustness

1. Introduction

Several finite element methods have been proposed in the last years in order to take into account discontinuities which are not necessarily aligned with the mesh. One of them is NXFEM (Nitsche's eXtended Finite Element Method), introduced by A. Hansbo and P. Hansbo in [13] and based on the use of Nitsche's

*Corresponding author

Email addresses: `daniela.capatina@univ-pau.fr` (D. Capatina),
`hammou.el-otmany@univ-pau.fr` (H. El-Otmany), `didier.graebling@univ-pau.fr` (D. Graebling), `robert.luce@univ-pau.fr` (R. Luce)

method to treat the transmission conditions on the interface. This method is also called "unfitted FEM" or "CutFEM". It uses standard finite element spaces, which are enriched on the cells cut by the interface, such that the degrees of freedom are doubled on these cells. Some recent developments of NXFEM
10 concern its robustness with respect to both the geometry and the physical coefficients, see for instance [2, 1], or its application to different model problems, such as fluid flow or fluid-structure interaction, cf. for instance [6, 8, 16, 15].

We mainly focus in this work on an elliptic equation with discontinuous coefficients across an interface. NXFEM has mostly been used so far with continuous finite elements; variants for discontinuous Galerkin approximations can
15 be found in [3, 17]. The goal of the present paper is to extend it to the case of nonconforming elements on triangular meshes, without any loss of robustness. These elements are widely used due to their small stencil and to the fact that they satisfy the inf-sup condition for Stokes equations.

For P^1 -continuous elements, the degrees of freedom are associated to the nodes, which belong to only one of the sub-domains delimited by the interface. Meanwhile, the degrees of freedom of the Crouzeix-Raviart P^1 -nonconforming elements [9] are associated to the edges, so those associated to the cut edges
20 belong to two sub-domains simultaneously. Due to this feature, a direct application of the NXFEM principle, which consists in doubling the degrees of freedom on the cut cells, does not allow to optimally bound the consistency error.

To overcome the previous difficulty, we propose two approaches. The first one consists in keeping the classical Crouzeix-Raviart space and in adding stabilisation on the cut edges, inspired by the discontinuous Galerkin method with
30 interior penalty. The method thus becomes consistent on the cut cells. The second approach consists in modifying the nonconforming basis functions on the cut triangles, by associating their degrees of freedom no longer to the whole edges but to the segments of cut edges. The consistency error on the cut cells has now an optimal convergence order, and stabilisation is only employed on
35 the interface, as in the conforming NXFEM.

[Both methods yield uniformly stable discrete problems, with respect to the](#)

position of the interface and the diffusion coefficients simultaneously. The uniform coercivity and continuity of the bilinear forms further imply that the condition numbers are robust, too. Note that in the original conforming NXFEM [13], only the robustness with respect to the position of the interface was considered; by introducing judicious weights, a uniformly stable variant with respect to both the geometry and the coefficients is proposed in [2, 1].

In this paper, we are mostly interested in another important feature of NXFEM, the robustness of the error estimate with respect to the position of the interface and the diffusion coefficients. For this purpose, the standard approach is to study the interpolation error, and then use the Céa or the Strang lemmas. As regards the conforming case, the H^1 -interpolation error is robust, see [13] but, to the best of our knowledge, there is no theoretical proof for the robustness in energy norm. Indeed, the interface term can be uniformly bounded with respect to either the position of the interface or the diffusion coefficients (see Section 2), but not to both of them simultaneously.

Under a non-restrictive hypothesis on the interface, we prove that the two nonconforming methods have the same behaviour with respect to the position of the interface and the diffusion coefficients as the conforming one. We next focus on the modifications due to the use of nonconforming finite elements.

For the first nonconforming method, we apply Strang's lemma in order to establish the robustness. Since one can use a well-known interpolation operator (here, the Crouzeix-Raviart one), then one only has to bound the additional term (in comparison to the conforming case) which appears in the interpolation error. This term results from the stabilisation on the cut edges and the proof of its robustness is direct. It relies on a precise trace inequality, written on a triangular part of a cut cell instead of the whole cell.

As regards the second nonconforming method, we have managed to prove its robustness by considering, for a theoretical purpose only, a NXFEM formulation written on completely discontinuous spaces. The latter has exactly the same stabilisation terms on the cut edges as the first nonconforming formulation, and therefore the same robustness. By passing to the limit as the stabilisation

parameters tend to infinity in this discontinuous Galerkin problem, we retrieve our nonconforming method with modified basis functions. Since the constant
70 in the dG error estimate is independent of the stabilisation parameters, the passage to the limit yields the desired robustness for the nonconforming limit problem, too. This approach allowed us to avoid the study of the interpolation error for the modified elements on the cut cells, which rises a technical difficulty (see the Appendix).

75 We also propose without any proof an extension to Stokes equations, which uses the modified Crouzeix-Raviart elements for the velocity and piecewise constant elements for the pressure. Stabilisation is added only on the interface, contrarily to the other NXFEM methods for the interface Stokes problem in the literature, cf. for instance [4, 7, 14]. The numerical tests are in agreement with
80 the expected theoretical results of stability and convergence.

The outline of the paper is as follows. Section 2 contains the employed notation and the presentation of NXFEM with conforming finite elements. In Section 3, we introduce and study the nonconforming method with additional stabilisation. Section 4 is devoted to the analysis of the nonconforming method
85 with modified Crouzeix-Raviart elements. Numerical tests for the elliptic problem are shown in Section 5, whereas in Section 6, we consider a nonconforming approximation of the Stokes equations and we validate it numerically. Section 7 contains some concluding remarks. Finally, in the Appendix we discuss the H^1 - interpolation error for the second nonconforming method.

90 2. NXFEM with conforming finite elements

Let Ω be a bounded domain of \mathbb{R}^2 , with a polygonal boundary $\partial\Omega$ and an internal smooth boundary Γ dividing Ω into two open sets Ω^{in} and Ω^{ex} . We

consider the model problem:

$$\left\{ \begin{array}{ll} -\operatorname{div}(\mu \nabla u) & = f & \text{in } \Omega^{in} \cup \Omega^{ex} \\ u & = 0 & \text{on } \partial\Omega \\ [u] & = 0 & \text{on } \Gamma \\ [\mu \nabla u \cdot n] & = g & \text{on } \Gamma \end{array} \right. \quad (1)$$

where $f \in L^2(\Omega)$, $g \in L^2(\Gamma)$ and n is the unit normal to the interface Γ oriented from Ω^{in} towards Ω^{ex} . For the sake of simplicity, we suppose that μ is piecewise constant, discontinuous across Γ and taking the values μ_{in} and μ_{ex} in the sub-domains Ω^{in} and Ω^{ex} . We consider here homogeneous Dirichlet bound-
95 ary conditions; the treatment of more general ones does not rise any particular difficulty.

Let $(\mathcal{T}_h)_h$ be a regular family of triangulations of Ω , each \mathcal{T}_h consisting of triangles. As usual, we denote by h_T the diameter of the triangle T and we set $h = \max_{T \in \mathcal{T}_h} h_T$. We denote by $\mathcal{T}_h^\Gamma = \{T \in \mathcal{T}_h; T \cap \Gamma \neq \emptyset\}$ the set of cut cells and
100 we introduce $\mathcal{T}_h^i = \{T \in \mathcal{T}_h; T \cap \Omega^i \neq \emptyset\}$ and $\Omega_h^i = \cup_{T \in \mathcal{T}_h^i} T$, for $i = in, ex$. \mathcal{E}_h denotes the set of edges of \mathcal{T}_h , \mathcal{E}_h^{nc} the set of uncut edges of \mathcal{T}_h while $\mathcal{E}_h^{i, cut}$ denotes the set of cut segments contained in Ω^i . For any $T \in \mathcal{T}_h^\Gamma$, we set $\Gamma_T = T \cap \Gamma$ and $T^i = T \cap \Omega^i$, for $i = in, ex$. For a given side $e \in \mathcal{E}_h$, we fix once for all a unit normal n_e ; if e is situated on the boundary $\partial\Omega$, then n_e coincides
105 with the outward normal n_Ω .

For $x \in \Gamma$ and v a piecewise smooth function, we set

$$v^{in}(x) = \lim_{\varepsilon \rightarrow 0} v(x - \varepsilon n), \quad v^{ex}(x) = \lim_{\varepsilon \rightarrow 0} v(x + \varepsilon n)$$

and we define its jump across Γ as well as the following weighted means by:

$$[v] = v^{in} - v^{ex}, \quad \{v\} = k^{ex} v^{ex} + k^{in} v^{in}, \quad \{v\}_* = k^{in} v^{ex} + k^{ex} v^{in},$$

where the weights satisfy $k^{in} + k^{ex} = 1$ and $0 < k^{in}, k^{ex} < 1$.

We denote by the letter c any constant independent of the discretisation, the diffusion coefficients and the position of the interface; we shall also use the notation $A \simeq B$ whenever $c_1 B \leq A \leq c_2 B$.

We next recall the NXFEM formulation of (1), introduced in [13] for a piecewise linear, continuous finite element approximation on a mesh of Ω which is not aligned with the interface Γ . The idea is to use standard finite element spaces but to double the degrees of freedom on the cut cells, and to treat the transmission conditions on Γ weakly, by means of Nitsche's method [18].

Let the finite dimensional spaces:

$$W_h^i = \{v \in H^1(\Omega_h^i); v|_T \in P^1, \forall T \in \mathcal{T}_h^i, v|_{\partial\Omega} = 0\}, \quad i = in, ex,$$

and let the product space $W_h = W_h^{in} \times W_h^{ex}$. Let us introduce:

$$\begin{aligned} a_h(u_h, v_h) &= \int_{\Omega^{in} \cup \Omega^{ex}} \mu \nabla u_h \cdot \nabla v_h dx - \int_{\Gamma} \{\mu \nabla u_h \cdot n\} [v_h] ds \\ &\quad - \int_{\Gamma} \{\mu \nabla v_h \cdot n\} [u_h] ds + \lambda \sum_{T \in \mathcal{T}_h^{\Gamma}} \int_{\Gamma_T} \lambda_T [u_h] [v_h] ds, \\ l_h(v_h) &= \int_{\Omega} f v_h dx + \int_{\Gamma} g \{v_h\}_* ds, \end{aligned}$$

where $\lambda > 0$ is a stabilisation parameter and where the coefficients k^{in} , k^{ex} , λ_T are defined as follows:

$$k^{in} = \frac{\mu_{ex} |T^{in}|}{\mu_{ex} |T^{in}| + \mu_{in} |T^{ex}|}, \quad k^{ex} = \frac{\mu_{in} |T^{ex}|}{\mu_{ex} |T^{in}| + \mu_{in} |T^{ex}|}, \quad \lambda_T = \frac{\mu_{in} \mu_{ex} |\Gamma_T|}{\mu_{in} |T^{ex}| + \mu_{ex} |T^{in}|}.$$

We use here above the expressions proposed in [2, 1], inspired by the discontinuous Galerkin method with discontinuous coefficients [11]; contrarily to the original weighting proposed in [13], they also take into account the geometry of the cut cells **and lead to a robust condition number**. The discrete problem reads:

$$\bar{u}_h \in W_h, \quad a_h(\bar{u}_h, v_h) = l_h(v_h), \quad \forall v_h \in W_h. \quad (2)$$

We consider the following norms on $H_0^1(\Omega) \cap H^2(\Omega^{ex} \cup \Omega^{in})$:

$$\begin{aligned} \|v\|_h^2 &= \sum_{i=in,ex} |\mu_i^{1/2} v|_{1,\Omega^i}^2 + \sum_{T \in \mathcal{T}_h^{\Gamma}} \lambda_T \| [v] \|_{0,\Gamma_T}^2, \\ \| |v| \|_h^2 &= \|v\|_h^2 + \sum_{T \in \mathcal{T}_h^{\Gamma}} \frac{|\Gamma_T|}{\lambda_T h_T} \| \{\mu \partial_n v\} \|_{0,\Gamma_T}^2. \end{aligned} \quad (3)$$

It is important to note that the two norms are equivalent on finite dimensional spaces, uniformly with respect to both the mesh-interface geometry and to the diffusion parameters. Indeed, we have:

$$\|\{\mu\partial_n v_h\}\|_{0,\Gamma_T} \leq \sum_{i=in,ex} \|k^i \mu_i \partial_n v_h\|_{0,\Gamma_T} \leq \sum_{i=in,ex} \sqrt{\frac{\lambda_T |T^i|}{|\Gamma_T|}} \|\mu_i^{1/2} \partial_n v_h\|_{0,\Gamma_T}, \quad (4)$$

thanks to $0 \leq \sqrt{k^i} \leq 1$ and to $k^i \mu_i = \lambda_T |T^i| / |\Gamma_T|$. The desired equivalence follows by using $|T^i| \leq ch_T^2$ and the trace inequality [13] on a cut cell $T \in \mathcal{T}_h^\Gamma$:

$$\frac{1}{\sqrt{h_T}} \|\varphi\|_{0,\Gamma_T} \leq c \left(\frac{1}{h_T} \|\varphi\|_{0,T} + |\varphi|_{1,T} \right), \quad \forall \varphi \in H^1(T), \quad (5)$$

115 with a constant c independent of h and Γ_T .

The $(W_h, \|\cdot\|_h)$ -stability for λ sufficiently large was established in [2, 1], uniformly with respect to both the mesh-interface geometry and to the diffusion parameters. Hence, the uniform stability with respect to $\|\cdot\|_h$ also holds. The consistency of (2) can be found in [13], as well as the global interpolation operator $L_h = (L_h^{in}, L_h^{ex}) : H^2(\Omega^{in}) \times H^2(\Omega^{ex}) \rightarrow W_h^{in} \times W_h^{ex}$ defined by:

$$v|_{\Omega^i} \rightarrow E^i v|_{\Omega} \rightarrow (L_h^* \circ E^i) v|_{\Omega} \rightarrow (L_h^* \circ E^i) v|_{\Omega_h^i} =: L_h^i v, \quad i = in, ex. \quad (6)$$

Here above, E^i denotes a continuous extension operator from $H^2(\Omega^i)$ to $H^2(\Omega)$ and L_h^* is the Lagrange interpolation operator associated to the mesh \mathcal{T}_h of Ω .

This yields *a priori* error estimates in the norm $\|\cdot\|_h$, which are optimal with respect to h and robust with respect to the diffusion coefficients. The H^1 -
120 interpolation error is also robust with respect to the position of the interface.

However, to the best of our knowledge, there is no theoretical proof of a robust bound for the interface term $\lambda_T^{1/2} \|[v - L_h v]\|_{0,\Gamma_T}$. One can for instance bound λ_T as follows:

$$\lambda_T = \frac{|\Gamma_T|}{\frac{|T^{in}|}{\mu_{in}} + \frac{|T^{ex}|}{\mu_{ex}}} \leq \frac{|\Gamma_T| \mu_i}{|T^i|}, \quad i = in, ex.$$

By using the trace inequality (5), one then ends up with

$$\lambda_T^{1/2} \|[v - L_h v]\|_{0,\Gamma_T} \leq ch_T \sum_{i=in,ex} \sqrt{\frac{|\Gamma_T| h_T}{|T^i|}} |\mu_i^{1/2} E^i v^i|_{2,T}, \quad (7)$$

which is robust with respect to the diffusion coefficients but not to the position of Γ . Indeed, the coefficient $\frac{|\Gamma_T| h_T}{|T^i|}$ may blow up when Γ_T is close to an edge or a node. However, if Γ_T is close to a node and the triangular part of the cut cell T is not degenerate, the estimate (7) can be improved and rendered uniform
125 with respect to Γ_T , as it will be discussed in 5.2.

Remark 1. *Another possibility is to use that $|T^{in}| + |T^{ex}| = |T|$ in order to bound λ_T differently:*

$$\lambda_T = \frac{|\Gamma_T|}{\frac{|T^{in}|}{\mu_{in}} + \frac{|T^{ex}|}{\mu_{ex}}} \leq \frac{|\Gamma_T|}{|T|} \max\{\mu_{in}, \mu_{ex}\}.$$

This leads to an interpolation error with a constant independent of the position of Γ , but depending now on the ratio between the diffusion coefficients.

Remark 2. *Nevertheless, according to the numerical experiments reported in the literature, the previous NXFEM method seems to be quite robust with respect
130 to both the position of the interface and the diffusion coefficients. This behaviour is confirmed by the numerical tests of subsection 5.2.*

Remark 3. *For the sake of simplicity, we assume in what follows that Γ_T is a segment on each cut cell T . This hypothesis is only used in the proofs of Theorem 1 and Proposition 1, where we need to express the measures of the cut parts T^{in}
135 and T^{ex} of T . If Γ_T is curved, all the results still hold true if $|T^i| \simeq |T_h^i|$, where T_h^{in}, T_h^{ex} are obtained by cutting T with the line $\Gamma_{T,h}$, which has the same ends as Γ_T .*

3. Nonconforming NXFEM with additional stabilisation

In what follows, we are interested in the discretization of (1) by Crouzeix-Raviart nonconforming elements [9]. The finite element space associated to the triangulation \mathcal{T}_h^i (of sides \mathcal{E}_h^i) is now

$$V_h^i = \left\{ \varphi \in L^2(\Omega_h^i); \varphi|_T \in P^1, \forall T \in \mathcal{T}_h^i, \int_e [\varphi] ds = 0, \forall e \in \mathcal{E}_h^i \right\},$$

where $[\cdot]$ denotes here the jump across e ; on a boundary side, the jump is equal
140 to the trace. We introduce the product space $V_h = V_h^{in} \times V_h^{ex}$ and we define a

global interpolation operator $I_h = (I_h^{in}, I_h^{ex})$ following the approach (6) of the conforming case. This ensures $\int_e (I_h^i v - v) ds = 0$ on any edge $e \in \mathcal{E}_h^i$, but this property does not hold on the segments of cut edges $e \in \mathcal{E}_h^{i,cut}$.

In order to balance the consistency error on the cut edges, we propose to
 145 add some stabilisation terms in the weak formulation. They are inspired by the discontinuous Galerkin method with symmetric interior penalty (see for instance [10]) but they have specific weights, which take into account the geometry of the cut cells.

Remark 4. Thanks to the consistency on the cut edges, one can still use the
 150 interpolation operator $I_h = (I_h^{in}, I_h^{ex})$ since the property $\int_e (I_h^i v - v) ds = 0$ on $e \in \mathcal{E}_h^{i,cut}$ is no longer necessary.

We introduce the following stabilisation forms on $V_h^i \times V_h^i$, for $i = in, ex$:

$$\begin{aligned} A^i(u_h, v_h) &= - \sum_{e \in \mathcal{E}_h^{i,cut}} \int_e (\{\mu \partial_n u_h\}_e [v_h] + \{\mu \partial_n v_h\}_e [u_h]) ds, \\ J^i(u_h, v_h) &= \sum_{e \in \mathcal{E}_h^{i,cut}} \mu_i \gamma_e^i \int_e [\pi_e^0 u_h] [\pi_e^0 v_h] ds, \quad \gamma_e^i = \frac{|e|}{|T^{l,i}| + |T^{r,i}|} \end{aligned}$$

where π_e^0 is the $L^2(e)$ -orthogonal projection on $P^0(e)$. The new bilinear form of the problem is defined on $V_h \times V_h$ by:

$$A_h(u_h, v_h) = a_h(u_h, v_h) + \sum_{i=in, ex} (A^i(u_h, v_h) + \gamma^i J^i(u_h, v_h)), \quad (8)$$

where $\gamma^i > 0$ are stabilisation parameters independent of h . The notation $\{\cdot\}_e$ stands for the following weighted mean on the segments of cut edges $e \in \mathcal{E}_h^{i,cut}$:

$$\{\phi\}_e = \kappa^l \phi^l + \kappa^r \phi^r, \quad \kappa^l = \frac{|T^{l,i}|}{|T^{l,i}| + |T^{r,i}|}, \quad \kappa^r = \frac{|T^{r,i}|}{|T^{l,i}| + |T^{r,i}|}.$$

Here above, T^r and T^l denote the two cut triangles whose common boundary contains e . If e is situated on $\partial\Omega$, then $\{\cdot\}_e$ is equal to the trace.

For $e \in \mathcal{E}_h^{i,cut}$ a segment of a whole edge $E \in \mathcal{E}_h$, we introduce the ratio
 155 $\alpha_e = \frac{|e|}{|E|}$. It is useful to introduce the similar ratios α_e^l and α_e^r for the other cut segments of $T^{l,i}$ and $T^{r,i}$ respectively, see Figure 1 (b).

In this section, we assume, whenever both $T^{l,i}$ and $T^{r,i}$ are triangles, that

$$\frac{\alpha_e}{\alpha_e^l + \alpha_e^r} \leq c, \quad \forall e \in \mathcal{E}_h^{i,cut}, \quad i = in, ex. \quad (9)$$

Remark 5. Condition (9) is satisfied, for instance, if $\alpha_e \simeq \alpha_e^l$ or $\alpha_e \simeq \alpha_e^r$, whether these values tend towards 0 or not. The critical case when $\frac{\alpha_e}{\alpha_e^l + \alpha_e^r} \rightarrow \infty$ and both $T^{l,i}, T^{r,i}$ are triangles looks like a rather pathological one, and it occurs when Γ_{T^l} and Γ_{T^r} nearly coincide with the common edge of the triangles T^l and T^r . A forbidden situation where both the triangles $T^{l,i}, T^{r,i}$ degenerate is shown in Figure 1 (b).

Remark 6. We have chosen to use a minimal stabilisation on the cut edges for this nonconforming approximation, which involves the jump of the piecewise constant projection $[\pi_e^0(\cdot)]$. We refer to [5] for a complete analysis. Of course, one can also employ the whole jump $[\cdot]$ in the bilinear form $J^i(\cdot, \cdot)$.

The approximation space V_h is endowed with the following norm:

$$[[v_h]]^2 = |||v_h|||_h^2 + \sum_{i=in,ex} J^i(v_h, v_h).$$

The discrete variational formulation of (1) is given by:

$$U_h \in V_h, \quad A_h(U_h, v_h) = l_h(v_h), \quad \forall v_h \in V_h. \quad (10)$$

The choice of κ^l, κ^r and γ_e^i allows to establish the following bound.

Lemma 1. Let $e \in \mathcal{E}_h^{i,cut}$ contained in the common boundary of two adjacent cut triangles T^l, T^r . Then one has, with $\mu = \mu_i$:

$$\| \{ \mu \partial_n v_h \} \|_{0,e}^2 \leq \mu \gamma_e^i \left(|\mu^{1/2} v_h|_{1,T^{l,i}}^2 + |\mu^{1/2} v_h|_{1,T^{r,i}}^2 \right), \quad \forall v_h \in V_h^i.$$

Proof. Since $\mu \nabla v_h$ is piecewise constant, $0 \leq \kappa^j \leq 1$ for $j = l, r$ and $\kappa^l + \kappa^r = 1$, we get by means of the Cauchy-Schwarz inequality that:

$$\begin{aligned} \int_e \{ \mu \partial_n v_h \}^2 ds &\leq \sum_{j=l,r} \mu \kappa^j \int_e \mu |\nabla v_h|_{T^j}^2 ds = \sum_{j=l,r} \frac{\mu \kappa^j |e|}{|T^{j,i}|} \int_{T^{j,i}} \mu |\nabla v_h|^2 ds \\ &= \frac{\mu |e|}{|T^{l,i}| + |T^{r,i}|} \sum_{j=l,r} \int_{T^{j,i}} \mu |\nabla v_h|^2 ds, \end{aligned}$$

which is exactly the stated result. \square

170 From Lemma 1 it follows that $A_h(\cdot, \cdot)$ is $[[\cdot]]$ -continuous and, for λ , γ^{in} and γ^{ex} sufficiently large, it is uniformly coercive on $V_h \times V_h$. Therefore, the discrete problem (10) is well-posed and Strang's lemma yields the error estimate:

$$[[u - U_h]] \leq c \left(\inf_{v_h \in V_h} [[u - v_h]] + \sup_{v_h \in V_h} \frac{|A_h(u - U_h, v_h)|}{[[v_h]]} \right), \quad (11)$$

with a constant c independent of h , μ and Γ .

We show next that the proposed nonconforming method exhibits the same
175 global robustness as the conforming one.

As regards the consistency error, we have:

$$A_h(u - U_h, v_h) = \sum_{e \in \mathcal{E}_h^{nc}} \int_e \mu \partial_n u [v_h] ds, \quad v_h \in V_h.$$

Its estimate is completely standard, since it involves only non-cut edges. By means of the Cauchy-Schwarz and the trace inequalities, together with Crouzeix-Raviart interpolation results, one classically gets that:

$$|A_h(u - U_h, v_h)| \leq ch |\mu^{1/2} u|_{2, \Omega^{in} \cup \Omega^{ex}} [[v_h]].$$

It remains to bound the interpolation error in (11), by means of the operator $I_h = (I_h^{in}, I_h^{ex})$. We next discuss the robustness for each term of the norm $[[\cdot]]$. The H^1 -error is robust because it can be bounded exactly as in the conforming case. The interpolation error of the normal derivative term on Γ is also robust;
180 this follows by applying first (4) to $u - I_h u$ and then (5) to $\nabla(u - I_h u)$. The jump term on the interface is bounded as in the conforming case, see Section 2.

In what follows, we focus on the additional term in the norm $[[\cdot]]$, due to the stabilisation on the cut edges. We show that it is robust under a non-restrictive assumption (9) on the interface Γ .

Theorem 1. *Let any $v \in H_0^1(\Omega) \cap H^2(\Omega^{in}) \times H^2(\Omega^{ex})$. Under the assumption (9), there exists a constant $c > 0$ independent of h , μ and Γ such that:*

$$\left(\sum_{i=in,ex} J^i(v - I_h^i v, v - I_h^i v) \right)^{1/2} \leq ch \sum_{i=in,ex} |\mu^{1/2} v|_{2, \Omega^i}.$$

Proof. We recall that, for $i = in, ex$,

$$J^i(v - I_h^i v, v - I_h^i v) = \sum_{e \in \mathcal{E}_h^{i, cut}} \mu_i \gamma_i^e \|\pi_e^0(v - I_h^i v)\|_{0,e}^2.$$

185 Let $e \in \mathcal{E}_h^{i, cut}$ a segment of a whole edge $E \in \mathcal{E}_h$ with $|e| = \alpha_e |E|$. Assume that E belongs to the adjacent cut triangles T^r and T^l ; the proof is completely similar if E is a boundary edge.

We begin by writing that:

$$\sqrt{\mu_i \gamma_i^e} \|\pi_e^0(v - I_h^i v)\|_{0,e} \leq \sqrt{\frac{\mu_i |e|}{|T^{l,i}| + |T^{r,i}|}} \sum_{j=l,r} \|(v - I_h^i v)|_{T^j}\|_{0,e}$$

and by applying next the trace inequality on the whole edge E . We thus obtain:

$$\begin{aligned} \sqrt{\mu_i \gamma_i^e} \|\pi_e^0(v - I_h^i v)\|_{0,e} &\leq \sqrt{\frac{\mu_i |e| |E|}{|T^{l,i}| + |T^{r,i}|}} \sum_{j=l,r} \frac{1}{\sqrt{|E|}} \|(v - I_h^i v)|_{T^j}\|_{0,E} \\ &\leq c \sqrt{\frac{\mu_i |e| |E|}{|T^{l,i}| + |T^{r,i}|}} \sum_{j=l,r} \left(\frac{1}{h_{T^j}} \|E^i v - I_h^i v\|_{0,T^j} + |E^i v - I_h^i v|_{1,T^j} \right) \\ &\leq ch \sqrt{\frac{\alpha_e |E|^2}{|T^{l,i}| + |T^{r,i}|}} |\mu_i|^{1/2} E^i v|_{2, T^l \cup T^r}. \end{aligned} \tag{12}$$

In order to discuss the robustness of the previous estimate with respect to the position of Γ , we distinguish between two cases.

190 If at least one of $T^{l,i}$, $T^{r,i}$ is a quadrilateral, let's say $T^{l,i}$, then we have:

$$|T^{l,i}| = |T^l| (1 - (1 - \alpha_e)(1 - \alpha_e^l)) \geq |T^l| \frac{\alpha_e + \alpha_e^l}{2}$$

and the previous bound is robust since:

$$\frac{\alpha_e |E|^2}{|T^{l,i}| + |T^{r,i}|} \leq \frac{\alpha_e |E|^2}{|T^{l,i}|} \leq \frac{2\alpha_e h^2}{|T^l|(\alpha_e + \alpha_e^l)} \leq \frac{2|E|^2}{|T^l|} \leq c.$$

If both $T^{l,i}$ and $T^{r,i}$ are triangles then $|T^{j,i}| \simeq \alpha_e \alpha_e^j h^2$ for $j = l, r$, such that

$$\frac{\alpha_e |E|^2}{|T^{l,i}| + |T^{r,i}|} \leq \frac{c}{\alpha_e^l + \alpha_e^r}.$$

In view of (12), this bound is not sufficiently robust since it may blow up when both α_e^l and α_e^r tend to 0, independently of α_e . In what follows, we improve the robustness by means of a more precise trace inequality, on the cut segment e instead of the whole edge E .

For this purpose, let us consider the isosceles triangles $\tilde{T}^{r,i} \subset T^r$ and $\tilde{T}^{l,i} \subset T^l$ of edge e as in Figure 1 (a). For each $j = l, r$, we first pass from T^j to the reference element \hat{T} by means of an affine transformation F_T^{-1} and then we consider the mapping $F_\alpha = \frac{1}{\alpha_e} F_T^{-1}$. Thus, one has that $F_\alpha(\tilde{T}^{j,i}) = \hat{T}$ and, with $\hat{x} = F_\alpha x$ and $\hat{\phi}(\hat{x}) = \phi(x)$, that:

$$|\hat{v}|_{1,\hat{T}} \simeq |v|_{1,\tilde{T}^{j,i}}, \quad \|\hat{v}\|_{0,\hat{T}} \simeq \frac{1}{\alpha_e h_T} \|v\|_{0,\tilde{T}^{j,i}}, \quad \forall v \in H^1(\tilde{T}^{j,i}).$$

Then the trace theorem on \hat{T} yields, with a constant independent of α_e :

$$\frac{1}{\sqrt{|\hat{e}|}} \|v\|_{0,e} = \frac{1}{\sqrt{|\hat{e}|}} \|\hat{v}\|_{0,\hat{e}} \leq c \left(\|\hat{v}\|_{0,\hat{T}} + |\hat{v}|_{1,\hat{T}} \right) \leq c \left(\frac{1}{\alpha_e h_T} \|v\|_{0,\tilde{T}^{j,i}} + |v|_{1,\tilde{T}^{j,i}} \right).$$

We next write that:

$$\|[\pi_e^0(v - I_h^i v)]\|_{0,e} \leq \sum_{j=l,r} \|\pi_{T^j}^0(E^i v - I_h^i v)\|_{0,e},$$

thanks to the properties of the projection operator π_e^0 and to the fact that $E^i v = v$ on e . By applying now the previous trace inequality to $\pi_{T^j}^0(E^i v - I_h^i v)$ on each $\tilde{T}^{j,i}$ and by using the properties of $\pi_{T^j}^0$, we get:

$$\begin{aligned} \sqrt{\mu_i \gamma_i^\varepsilon} \|[\pi_e^0(v - I_h^i v)]\|_{0,e} &\leq \sqrt{\frac{\mu_i \alpha_e^2 |E|^2}{|T^{l,i}| + |T^{r,i}|}} \sum_{j=l,r} \frac{1}{\sqrt{|e|}} \|\pi_{T^j}^0(E^i v - I_h^i v)\|_{0,e} \\ &\leq c \sqrt{\frac{\mu_i \alpha_e}{\alpha_e^l + \alpha_e^r}} \sum_{j=l,r} \frac{1}{\alpha_e h_{T^j}} \|\pi_{T^j}^0(E^i v - I_h^i v)\|_{0,\tilde{T}^{j,i}} \\ &\leq c \sqrt{\frac{\mu_i \alpha_e}{\alpha_e^l + \alpha_e^r}} \sum_{j=l,r} \frac{1}{h_{T^j}} \|\pi_{T^j}^0(E^i v - I_h^i v)\|_{0,T^j} \\ &\leq ch \sqrt{\frac{\alpha_e}{\alpha_e^l + \alpha_e^r}} |\mu_i^{1/2} E^i v|_{2,T^l \cup T^r}. \end{aligned}$$

195 Therefore, the estimate is robust under the assumption (9). Finally, we deduce the announced estimate thanks to the continuity of the extension operators $E^i : H^2(\Omega^i) \longrightarrow H^2(\Omega)$.

□

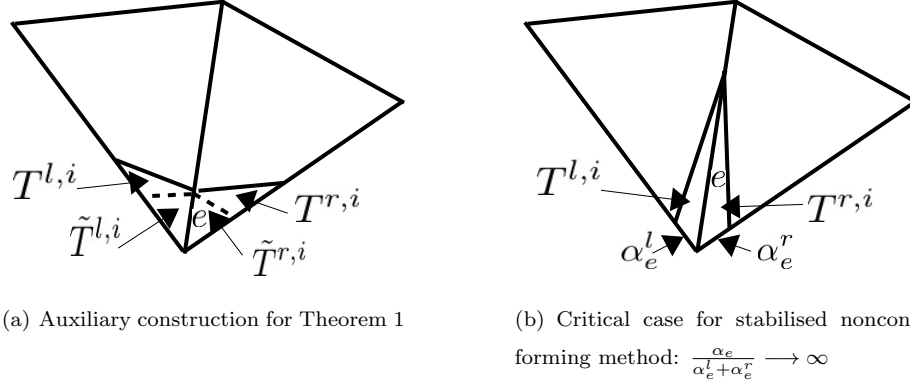


Figure 1: Two adjacent elements sharing an interior cut edge

In conclusion, by putting together the previous results, we obtain from (11)
 200 an error estimate for $[[u - U_h]]$ exactly as in the conforming method.

4. Nonconforming NXFEM with modified basis functions

In the following, we propose another nonconforming method, which does not need any further stabilisation in comparison to the conforming case.

4.1. Modified basis functions on the cut cells

205 To do so, we modify the Crouzeix-Raviart basis functions on the cut triangles by associating their degrees of freedom no longer to the whole edges, but to the segments of cut edges.

Let the triangle $T = (ABC) \in \mathcal{T}_h^\Gamma$, cut by Γ at the points $M \in (AC)$ and $N \in (BC)$. We set:

$$\frac{|AM|}{|AC|} = \alpha, \quad \frac{|BN|}{|BC|} = \beta, \quad 0 < \alpha, \beta < 1. \quad (13)$$

We denote by T^\square the quadrilateral part of T and by T^\triangle the triangular one, see Figure 2. We first look for the new basis functions $(\varphi_i^\square)_{1 \leq i \leq 3}$ associated to the segments $e_1^\square = AM$, $e_2^\square = BN$ and $e_3^\square = AB$ of T^\square . We impose:

$$\int_{e_j^\square} \varphi_i^\square ds = |e_j^\square| \delta_{ij}, \quad \forall 1 \leq i, j \leq 3 \quad (14)$$

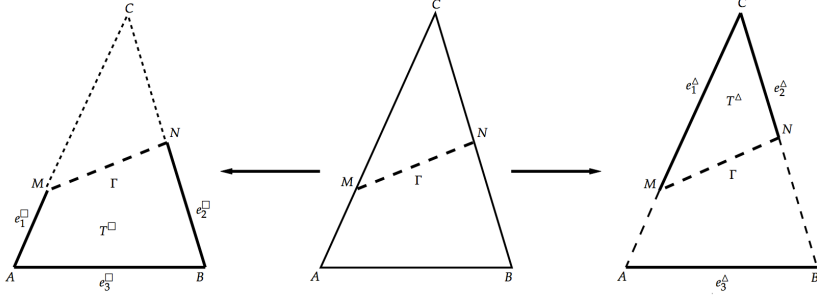


Figure 2: Triangle (ABC) cut by Γ

where δ_{ij} is the Kronecker symbol.

We decompose each $\varphi_i^\square \in P^1(T)$ in the standard Crouzeix-Raviart basis $\{\varphi_j\}_{1 \leq j \leq 3}$ as follows: $\varphi_i^\square = \sum_{j=1}^3 a_{ij}^\square \varphi_j$ and we next determine a_{ij}^\square . For the computation of the integrals in (14), we use the values of φ_j at the midpoints M^\square , N^\square of $e_1^\square = AM$ and $e_2^\square = BN$ respectively. Since their coordinates are

$$x_{M^\square} = \frac{\alpha}{2}x_C + \left(1 - \frac{\alpha}{2}\right)x_A, \quad x_{N^\square} = \frac{\beta}{2}x_C + \left(1 - \frac{\beta}{2}\right)x_B,$$

we immediately get:

$$\begin{aligned} \varphi_1(M^\square) &= 1, & \varphi_2(M^\square) &= \alpha - 1, & \varphi_3(M^\square) &= 1 - \alpha, \\ \varphi_1(N^\square) &= \beta - 1, & \varphi_2(N^\square) &= 1, & \varphi_3(N^\square) &= 1 - \beta. \end{aligned}$$

After some simple computations, we finally obtain:

$$\begin{aligned} \varphi_1^\square &= \frac{1}{1 - (1 - \alpha)(1 - \beta)}\varphi_1 + \frac{1 - \beta}{1 - (1 - \alpha)(1 - \beta)}\varphi_2, \\ \varphi_2^\square &= \frac{1 - \alpha}{1 - (1 - \alpha)(1 - \beta)}\varphi_1 + \frac{1}{1 - (1 - \alpha)(1 - \beta)}\varphi_2, \\ \varphi_3^\square &= \frac{-(1 - \alpha)(2 - \beta)}{1 - (1 - \alpha)(1 - \beta)}\varphi_1 - \frac{(2 - \alpha)(1 - \beta)}{1 - (1 - \alpha)(1 - \beta)}\varphi_2 + \varphi_3. \end{aligned} \tag{15}$$

In order to determine the basis functions $(\varphi_i^\Delta)_{1 \leq i \leq 3}$ associated to the segments $e_1^\Delta = CM$, $e_2^\Delta = CN$ and $e_3^\Delta = AB$ of T^Δ , it is now sufficient to replace

in (15) $\alpha - 1$ and $\beta - 1$ by α and β respectively, which yields:

$$\begin{aligned}\varphi_1^\Delta &= \frac{1}{1-\alpha\beta}\varphi_1 - \frac{\beta}{1-\alpha\beta}\varphi_2, & \varphi_2^\Delta &= -\frac{\alpha}{1-\alpha\beta}\varphi_1 + \frac{1}{1-\alpha\beta}\varphi_2, \\ \varphi_3^\Delta &= \frac{\alpha(1-\beta)}{1-\alpha\beta}\varphi_1 + \frac{\beta(1-\alpha)}{1-\alpha\beta}\varphi_2 + \varphi_3.\end{aligned}\tag{16}$$

Remark 7. Note that the previous basis functions depend only on the position of the intersection points of T with Γ , and not of the curvature of the interface. Moreover, one has that $\varphi_1^\Delta + \varphi_2^\Delta + \varphi_3^\Delta = \varphi_1^\square + \varphi_2^\square + \varphi_3^\square = \varphi_1 + \varphi_2 + \varphi_3 = 1$.

It is easy to check that $(\varphi_1^\square, \varphi_2^\square, \varphi_3^\square)$ is a basis of $P^1(T)$ and therefore (T, P^1, Σ^\square) is a finite element, where Σ^\square denotes the set of degrees of freedom defined in (14). It goes the same way for (T, P^1, Σ^Δ) .

We can now introduce the new approximation space $\tilde{V}_h = \tilde{V}_h^{in} \times \tilde{V}_h^{ex}$, where the basis functions of \tilde{V}_h^i are the classical Crouzeix-Raviart functions on the non-cut cells and the previously defined functions on the cut cells.

The discrete problem reads:

$$u_h \in \tilde{V}_h, \quad a_h(u_h, v_h) = l_h(v_h), \quad \forall v_h \in \tilde{V}_h.\tag{17}$$

The proof of the uniform $(\tilde{V}_h, ||| \cdot |||_h)$ -stability of $a_h(\cdot, \cdot)$ is completely similar to the conforming case. The stability yields the well-posedness of (17), the robustness of the condition number as well as standard *a priori* error estimate in the norm $||| \cdot |||_h$, similar to (11).

4.2. Robustness with respect to the position of the interface

In the following, we prove that the error $|||u - u_h|||_h$ exhibits the same robustness with respect to the position of Γ as the conforming method.

For this purpose, we first introduce a formulation similar to (10) but written on completely discontinuous spaces, and then we pass to the limit on the stabilisation parameters and obtain the formulation (17). Its robustness follows from the robustness results of Section 3 extended to the DG fomulation. Let

$$D_h^i = \{v_h \in L^2(\Omega_h^i) : v_h|_T \in P^1(T), \forall T \in \mathcal{T}_h^i\}, \quad i = in, ex,$$

225 and let the following stabilisation terms on the non-cut edges (the same as in the symmetric discontinuous Galerkin method) interior penalty:

$$\begin{aligned} A^{DG}(u_h, v_h) &= - \sum_{e \in \mathcal{E}_h^{nc}} \int_e (\{\mu \nabla_n u_h\}[v_h] + \{\mu \nabla_n v_h\}[u_h]) ds, \\ J^{DG}(u_h, v_h) &= \sum_{e \in \mathcal{E}_h^{nc}} \frac{1}{|e|} \int_e \mu [\pi_e^0 u_h][\pi_e^0 v_h] ds. \end{aligned}$$

Then we define on $D_h = D_h^{in} \times D_h^{ex}$ the bilinear form

$$A_h^{DG}(\cdot, \cdot) = A_h(\cdot, \cdot) + A^{DG}(\cdot, \cdot) + \gamma^{DG} J^{DG}(\cdot, \cdot),$$

with $\gamma^{DG} > 0$ a stabilisation parameter, and we consider the following DG approximation of (1):

$$u_h^\gamma \in D_h, \quad A_h^{DG}(u_h^\gamma, v_h) = l_h(v_h), \quad \forall v_h \in D_h. \quad (18)$$

The index $\gamma = (\gamma^{in}, \gamma^{ex}, \gamma^{DG})$ shows the dependence of the solution on the parameters. It is standard to show that (18) is well-posed for γ sufficiently large, with respect to the norm $(\|\cdot\|^2 + J^{DG}(\cdot, \cdot))^{1/2}$. A similar discontinuous Galerkin method for interface problems was analysed in [17]. Note that:

$$\begin{aligned} \text{Ker } J^i &= \left\{ v_h \in D_h^i; \int_e [v_h] ds = 0, \quad \forall e \in \mathcal{E}_h^{i,cut} \right\}, \quad i = in, ex, \\ \text{Ker } J^{DG} &= \left\{ v_h \in D_h; \int_e [v_h] ds = 0, \quad \forall e \in \mathcal{E}_h^{nc} \right\} \end{aligned}$$

and therefore, one has:

$$\left(\text{Ker } J^{in} \times \text{Ker } J^{ex} \right) \cap \text{Ker } J^{DG} = \tilde{V}_h^{in} \times \tilde{V}_h^{ex} = \tilde{V}_h. \quad (19)$$

Theorem 2. *Let u_h^γ and u_h the unique solutions of (18) and (17). Then*

$$\lim_{\gamma \rightarrow \infty} \left(\|[u_h^\gamma - u_h]\|^2 + J^{DG}(u_h^\gamma - u_h, u_h^\gamma - u_h) \right) = 0.$$

Proof. By taking the test-function $v_h = u_h^\gamma$ in (18), we get thanks to the continuity of $l_h(\cdot)$ and the coercivity of $A_h^{DG}(\cdot, \cdot)$ that:

$$\|[u_h^\gamma]\|^2 + J^{DG}(u_h^\gamma, u_h^\gamma) \leq c.$$

So $(u_h^\gamma)_\gamma$ is bounded in D_h , independently of γ . Consequently, there exists a subsequence, still denoted by $(u_h^\gamma)_\gamma$ which converges (weakly, and therefore strongly in D_h) towards u_h^∞ as $\gamma \rightarrow \infty$. According to (19), the limit u_h^∞ belongs to the modified nonconforming space \tilde{V}_h .

A passage to the limit in (18) yields that u_h^∞ satisfies the equation:

$$A_h^{DG}(u_h^\infty, v_h) = l_h(v_h), \quad \forall v_h \in \tilde{V}_h.$$

According to the definition of \tilde{V}_h , one has that:

$$J^{in}(u_h^\infty, v_h) = J^{ex}(u_h^\infty, v_h) = J^{DG}(u_h^\infty, v_h) = 0, \quad \forall v_h \in \tilde{V}_h.$$

Since $\partial_n u_h^\infty$ and $\partial_n v_h$ are constant on any edge $e \in \mathcal{E}_h^{in, cut} \cup \mathcal{E}_h^{ex, cut} \cup \mathcal{E}_h^{nc}$, one also has that:

$$A^{in}(u_h^\infty, v_h) = A^{ex}(u_h^\infty, v_h) = A^{DG}(u_h^\infty, v_h) = 0.$$

Thus, $A_h^{DG}(u_h^\infty, v_h) = a_h(u_h^\infty, v_h)$ for any $v_h \in \tilde{V}_h$ and therefore, u_h^∞ is solution to (17). The latter being well-posed, we deduce that $u_h^\infty = u_h$ and that all the sequence $(u_h^\gamma)_\gamma$ converges. \square

Remark 8. *If we pass to the limit as $(\gamma^{in}, \gamma^{ex})$ tend to infinity in the nonconforming formulation (10) instead of the discontinuous Galerkin one (18), then the limit u_h^∞ does not satisfy problem (17). This is due to the fact that:*

$$\text{Ker} J^i = \left\{ v_h \in V_h^i; \int_e [v_h] ds = 0, \quad \forall e \in \mathcal{E}_h^{i, cut} \right\} \subset \tilde{V}_h^i, \quad i = in, ex.$$

The above inclusion is strict because a function of $\text{Ker} J^i$ is continuous across any cut edge, whereas an element of \tilde{V}_h^i is only weakly continuous.

The discontinuous Galerkin formulation (18) has the same robustness as the stabilised nonconforming formulation (10). Indeed, they differ through the terms $A^{DG}(\cdot, \cdot)$ and $J^{DG}(\cdot, \cdot)$, which are written on the non-cut edges and which do not interfere with the position of the interface. Similarly to Section 3, we obtain under the non-restrictive assumption (9) the next error estimate for (18):

$$[[u_h^\gamma - u]] + J^{DG}(u_h^\gamma - u, u_h^\gamma - u)^{1/2} \leq Ch|u|_{2, \Omega^{in} \cup \Omega^{ex}},$$

where the dependence of C on the interface is the same as for the conforming method.

The constant C does not depend on the stabilisation parameters γ , as in any DG method. Therefore, we can pass to the limit as γ tends to infinity and deduce, thanks to Theorem 2, the error estimate for (10):

$$[[u_h - u]] \leq Ch|u|_{2,\Omega^{in} \cup \Omega^{ex}}.$$

5. Numerical tests

5.1. Convergence with respect to mesh refinement

We have implemented both nonconforming methods, with additional stabilisation and with modified basis functions. We show the convergence history for the following test-case, which was also considered in [13, 2]. Let $\Omega = (-1, 1) \times (-1, 1)$ and let Γ the circle of radius $r_0 = 3/4$ and of centre the origin, see Figure 3. The data are chosen such that

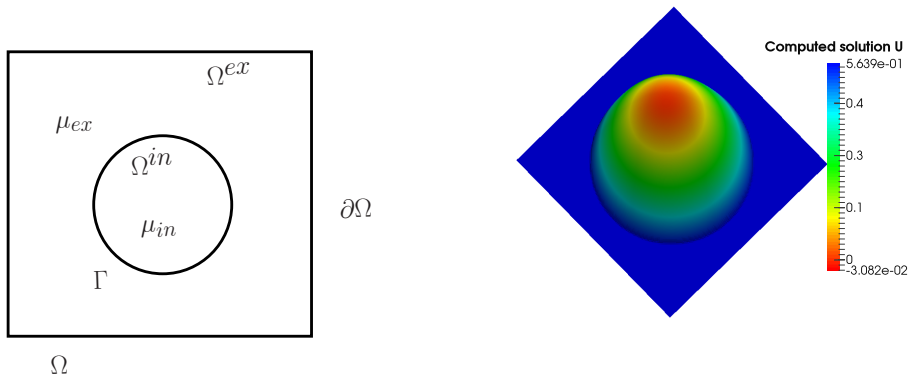


Figure 3: Geometry of the model problem and computed solution

$$u(x, y) = \begin{cases} \frac{r^2}{\mu_{ex}} & \text{if } r \leq r_0, \\ \frac{\mu_{in}}{r^2 - r_0^2} + \frac{r_0^2}{\mu_{in}} & \text{if } r > r_0 \end{cases}, \quad r = \sqrt{x^2 + y^2},$$

240 is an exact solution of (1) with Dirichlet conditions and with homogeneous
transmission conditions. The diffusion coefficients are $\mu_{in} = 1$ and $\mu_{ex} = 10^3$.
The solution on a mesh with $N = 65\,536$ elements is shown in Figure 3.

We show in Tables 1 and 2 the computed errors for the two methods (10)
and (17) respectively. We show the errors in energy and L^2 norms on a sequence
245 of uniformly refined meshes, as well as the convergence order computed from
the errors on two successively refined meshes (with N and $4N$ elements).

N	$[[u - U_h]]_h$	order	$\ u - U_h\ _{0,\Omega}$	order
64	3.95×10^{-1}	-	3.21×10^{-2}	-
256	1.67×10^{-1}	1.24	6.11×10^{-3}	2.39
1 024	7.91×10^{-2}	1.08	1.36×10^{-3}	2.16
4 096	4.81×10^{-2}	1.03	3.24×10^{-4}	2.07
16 384	1.98×10^{-2}	1.05	7.70×10^{-5}	2.07
65 536	9.87×10^{-3}	1.04	2.71×10^{-5}	2.05

Table 1: Convergence of the nonconforming approximation (10)

N	$ u - u_h _h$	order	$\ u - u_h\ _{0,\Omega}$	order
64	3.43×10^{-1}	-	3.13×10^{-2}	-
256	1.53×10^{-1}	1.163	5.40×10^{-3}	2.533
1 024	7.61×10^{-2}	1.007	1.28×10^{-3}	2.077
4 096	3.79×10^{-2}	1.007	3.20×10^{-4}	2.004
16 384	1.87×10^{-2}	1.021	7.63×10^{-5}	2.067
65 536	9.31×10^{-3}	1.007	1.90×10^{-5}	2.011

Table 2: Convergence of the nonconforming approximation (17)

This example has also been treated in [13] and [2] by means of conforming

finite elements. One can see in Table 3, the convergence rates for the conforming method of [2], with the same coefficients k^{in} , k^{ex} and λ_T as in the present paper. For the three considered methods, we numerically retrieve the optimal convergence orders $\mathcal{O}(N^{-1/2}) = \mathcal{O}(h)$ in the different energy norms, respectively $\mathcal{O}(N^{-1}) = \mathcal{O}(h^2)$ in the L^2 -norm. Moreover, the values of the errors in the three tables are very similar.

N	$\ u - \bar{u}_h\ _h$	order	$\ u - \bar{u}_h\ _{0,\Omega}$	order
64	3.45×10^{-1}	-	2.83×10^{-2}	-
256	1.68×10^{-1}	1.036	6.27×10^{-3}	2.176
1 024	8.03×10^{-2}	1.064	1.41×10^{-3}	2.154
4 096	3.95×10^{-2}	1.021	3.38×10^{-4}	2.060
16 384	1.97×10^{-2}	1.007	8.21×10^{-5}	2.039
65 536	9.82×10^{-3}	1.000	2.02×10^{-5}	2.021

Table 3: Convergence of the conforming approximation (2)

In the following, we focus only on the nonconforming method with modified basis functions, which does not need additional stabilisation on the cut edges.

5.2. Numerical robustness

The aim of this subsection is to illustrate the robustness of (17) with respect to the position of the interface, on a fixed mesh. In what follows, we have chosen to test a particular configuration where the interface is a straight line, and is close to a node or an edge on all the cut cells.

Let the domain $\Omega = (0, 1) \times (0, 1)$ and the interface $\Gamma_\varepsilon := x_\varepsilon \times [0, 1]$ depending on a parameter $\varepsilon > 0$. We consider a fixed triangulation, obtained by meshing Ω into 16×16 squares and by cutting next each square along a diagonal. We translate the interface by letting ε vary, such that the ratios α_T , β_T associated to any cut triangle T either decrease towards 0 or increase towards

1 simultaneously, see Figure 4. In this configuration, one has $\alpha_T = \beta_T$ so the triangular part T^Δ is not degenerate and implicitly, assumption (9) is satisfied.

According to the theoretical results, the critical term is the interpolation error related to the jump across Γ , see (7). This term appears in all NXFEM
 270 methods, independently of the chosen finite elements. On the triangular (non-degenerate) part T^Δ of a cut triangle T , one can use a trace theorem on T^Δ for $\frac{1}{\sqrt{|\Gamma_T|}} \|u - \tilde{I}_T^i u\|_{0,\Gamma_T}$ instead of the trace inequality (5) on T , similarly to the proof of Theorem 1. This technique allows to bound the previous error uniformly with respect to Γ_T . However, on the quadrilateral part T^\square , the
 275 constant $C(\Gamma) = \sqrt{\frac{|\Gamma_T| h_T}{|T^\square|}}$ involved in (7) behaves as $\frac{1}{\sqrt{\alpha_T + \beta_T}} \simeq \frac{1}{\sqrt{\alpha_T}}$, so it may blow up as α_T tends to 0.

We consider a test-case similar to one of [13]; the data are such that

$$u(x, y) = \begin{cases} \frac{x^2}{\mu_{in}} & \text{if } x \leq x_\varepsilon, \\ \frac{x^2 - x_\varepsilon^2}{\mu_{ex}} + \frac{x_\varepsilon^2}{\mu_{in}} & \text{if } x > x_\varepsilon, \end{cases}$$

is an exact solution of (1) with Dirichlet boundary conditions and with homogeneous interface conditions. In order to avoid any interference with the boundary conditions, we take $x_\varepsilon = \frac{1}{16} + \varepsilon$ which yields the critical value $\alpha_\varepsilon = 16\varepsilon$ on the
 280 quadrilateral part of a cut cell.

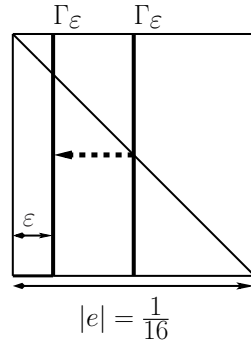


Figure 4: Variation of the position of the interface: zoom on a cut cell

We first take $\mu_{in} = 1$, $\mu_{ex} = 10$ and let ε vary, such that $\alpha_\varepsilon = 16\varepsilon$ varies

from 0.5, which corresponds to the ideal situation, to 10^{-5} . We compute several errors, both local (on the cut cells only) and global (on the whole domain), in order to check the sensitivity of the method with respect to the position of the interface. We denote:

$$|u - u_h|_*^2 = \sum_{T \in \mathcal{T}_h^\Gamma} \|\mu^{1/2} \nabla(u - u_h)\|_{0,T}^2, \quad \|u - u_h\|_*^2 = \sum_{T \in \mathcal{T}_h^\Gamma} \|u - u_h\|_{0,T}^2,$$

$$\|u - u_h\|_\Gamma^2 = \sum_{T \in \mathcal{T}_h^\Gamma} \lambda_T \| [u - u_h] \|_{0,T}^2.$$

Note that the solution itself depends on ε and hence, it varies when Γ_ε moves. We show in Table 4 the computed errors for different values of ε . One can note a slight increase of the error as ε decreases, but the method seems quite robust for small values of ε .

16ε	$ u - u_h _*$	$\ u - u_h\ _*$	$\ u - u_h\ _\Gamma$	$\ u - u_h\ _h$	$\ u - u_h\ _{0,\Omega}$
0.5	0.949×10^{-2}	2.920×10^{-4}	2.521×10^{-3}	1.134×10^{-1}	2.357×10^{-2}
10^{-1}	1.247×10^{-2}	4.244×10^{-4}	3.508×10^{-3}	1.137×10^{-1}	2.372×10^{-2}
10^{-2}	1.376×10^{-2}	4.722×10^{-4}	4.035×10^{-3}	1.139×10^{-1}	2.380×10^{-2}
10^{-3}	1.390×10^{-2}	4.773×10^{-4}	4.093×10^{-3}	1.139×10^{-1}	2.381×10^{-2}
10^{-4}	1.392×10^{-2}	4.778×10^{-4}	4.099×10^{-3}	1.139×10^{-1}	2.381×10^{-2}
10^{-5}	1.392×10^{-2}	4.779×10^{-4}	4.100×10^{-3}	1.139×10^{-1}	2.381×10^{-2}

Table 4: Errors versus position of the interface for $\mu_{in} = 1$, $\mu_{ex} = 10$

285 Furthermore, to test the robustness with respect to the diffusion coefficients, we now consider the case of highly discontinuous coefficients, $\mu_{in} = 0.1$ and $\mu_{ex} = 10^5$. Again, we move the interface by starting at $\alpha_\varepsilon = 0.5$ and by letting ε tend towards 0. The computed errors are given in Table 5.

290 We conclude that the method is numerically robust with respect to the position of Γ , independently of the ratio between the diffusion parameters.

16ε	$ u - u_h _*$	$\ u - u_h\ _*$	$\ u - u_h\ _\Gamma$	$\ u - u_h\ _h$	$\ u - u_h\ _{0,\Omega}$
0.5	1.561×10^{-2}	0.655×10^{-3}	0.698×10^{-2}	3.387×10^{-1}	2.399×10^{-2}
10^{-1}	3.559×10^{-2}	2.338×10^{-3}	1.229×10^{-2}	3.403×10^{-1}	2.393×10^{-2}
10^{-2}	4.080×10^{-2}	2.890×10^{-3}	1.388×10^{-2}	3.409×10^{-1}	2.396×10^{-2}
10^{-3}	4.133×10^{-2}	2.949×10^{-3}	1.405×10^{-2}	3.410×10^{-1}	2.397×10^{-2}
10^{-4}	4.139×10^{-2}	2.955×10^{-3}	1.407×10^{-2}	3.410×10^{-1}	2.397×10^{-2}
10^{-5}	4.140×10^{-2}	2.956×10^{-3}	1.407×10^{-2}	3.410×10^{-1}	2.397×10^{-2}

Table 5: Errors versus position of the interface for $\mu_{in} = 0.1$, $\mu_{ex} = 10^5$

6. Application to Stokes equations

The goal of this section is to solve numerically the Stokes equations with an interface, by using the previous nonconforming spaces with modified basis functions on the cut cells. We do not discuss here the mathematical analysis of the proposed formulation, which can be found in [12]; in the absence of any interface, it is well-known that the discrete problem is well-posed.

To our knowledge, only conforming finite elements have been employed so far for the Stokes interface problem in the context of NXFEM. Contrarily to the present formulation, all existing schemes need additional terms to ensure stability of the discrete mixed problem. We refer to [4], [7], [14] for such approximations, with different pairs of spaces for the velocity and the pressure.

We consider the incompressible flow of two immiscible Newtonian fluids with different viscosities, governed by the following Stokes equations:

$$\left\{ \begin{array}{ll} -\operatorname{div}(\mu \nabla \mathbf{u}) + \nabla p = \mathbf{f} & \text{in } \Omega^{in} \cup \Omega^{ex}, \\ \operatorname{div} \mathbf{u} = 0 & \text{in } \Omega^{in} \cup \Omega^{ex}, \\ \mathbf{u} = \mathbf{0} & \text{on } \partial\Omega, \\ [\mathbf{u}] = \mathbf{0} & \text{on } \Gamma, \\ [\mu \partial_n \mathbf{u} - p \mathbf{n}] = \mathbf{g} & \text{on } \Gamma, \end{array} \right. \quad (20)$$

where the viscosity is a positive constant in each sub-domain, $\mu|_{\Omega^i} = \mu_i$ for

$i = in, ex$, and where the data satisfy $\mathbf{f} \in L^2(\Omega)^2$, $\mathbf{g} \in L^2(\Gamma)^2$. For the sake of simplicity, we consider here homogeneous Dirichlet boundary conditions.

We introduce the spaces:

$$\mathbf{V} = H_0^1(\Omega)^2, \quad Q = \{p \in L^2(\Omega); \int_{\Omega} \mu^{-1} p \, dx = 0\},$$

and the following velocity-pressure formulation of (20): find $(\mathbf{u}, p) \in \mathbf{V} \times Q$,

$$\begin{cases} \mathbf{a}(\mathbf{u}, \mathbf{v}) + b(p, \mathbf{v}) &= \mathbf{l}(\mathbf{v}), \quad \forall \mathbf{v} \in \mathbf{V}, \\ b(q, \mathbf{u}) &= 0, \quad \forall q \in Q \end{cases} \quad (21)$$

where:

$$\begin{aligned} \mathbf{a}(\mathbf{u}, \mathbf{v}) &= \sum_{i=in,ex} \int_{\Omega^i} \mu \nabla \mathbf{u} : \nabla \mathbf{v} \, dx, & b(p, \mathbf{v}) &= \sum_{i=in,ex} \int_{\Omega^i} p \operatorname{div} \mathbf{v} \, dx, \\ \mathbf{l}(\mathbf{v}) &= \int_{\Omega} \mathbf{f} \cdot \mathbf{v} \, dx + \int_{\Gamma} \mathbf{g} \cdot \mathbf{v} \, ds. \end{aligned}$$

We propose to approximate the velocity by the $(P^1)^2$ -nonconforming elements modified on the cut cells, and the pressure by P^0 elements. Let $\tilde{\mathbf{V}}_h = \tilde{V}_h \times \tilde{V}_h$ and $Q_h = Q_h^{in} \times Q_h^{ex}$, where

$$Q_h^i = \{q \in L_0^2(\Omega^i); q|_T \in P^0(T), \forall T \in \mathcal{T}_h^i\}, \quad i = in, ex.$$

We introduce the following discrete variational formulation of (20), with no additional stabilization except the terms on Γ resulting from Nitsche's method for the interface conditions: find $(\mathbf{u}_h, p_h) \in \tilde{\mathbf{V}}_h \times Q_h$ such that

$$\begin{cases} \mathbf{a}_h(\mathbf{u}_h, \mathbf{v}_h) + b_h(p_h, \mathbf{v}_h) &= \mathbf{l}_h(\mathbf{v}_h), \quad \forall \mathbf{v}_h \in \tilde{\mathbf{V}}_h, \\ b_h(q_h, \mathbf{u}_h) &= 0, \quad \forall q_h \in Q_h \end{cases} \quad (22)$$

where:

$$\begin{aligned} \mathbf{a}_h(\mathbf{u}_h, \mathbf{v}_h) &= \sum_{i=in,ex} \int_{\Omega^i} \mu \nabla \mathbf{u}_h : \nabla \mathbf{v}_h \, dx - \int_{\Gamma} \{\mu \partial_n \mathbf{u}_h\} \cdot [\mathbf{v}_h] \, ds \\ &\quad - \int_{\Gamma} \{\mu \partial_n \mathbf{v}_h\} \cdot [\mathbf{u}_h] \, ds + \lambda \sum_{T \in \mathcal{T}_h^{\Gamma}} \lambda_T \int_{\Gamma_T} [\mathbf{u}_h] \cdot [\mathbf{v}_h] \, ds, \\ b_h(p_h, \mathbf{v}_h) &= - \sum_{i=in,ex} \int_{\Omega^i} p_h \operatorname{div} \mathbf{v}_h \, dx + \int_{\Gamma} \{p_h\} [\mathbf{v}_h \cdot \mathbf{n}] \, ds, \\ \mathbf{l}_h(\mathbf{v}_h) &= \int_{\Omega} \mathbf{f} \cdot \mathbf{v}_h \, dx + \int_{\Gamma} \mathbf{g} \cdot \{\mathbf{v}_h\}_* \, ds. \end{aligned}$$

305 The forms $\mathbf{a}_h(\cdot, \cdot)$ and $\mathbf{l}_h(\cdot)$ are the extensions to vector functions of those corresponding to the Darcy equations. The main difference with the Darcy discrete problem lies in the inf-sup condition for $b_h(\cdot, \cdot)$.

In what follows, we present some numerical tests in order to validate the formulation (22) from a numerical point of view. We consider two test-cases.

The first one is the same as in [4], where the authors solve a linear elasticity problem by means of a Stokes system. Let $\Omega = (0, 1) \times (0, 1)$ and Γ the circle of centre $(0.5, 0.5)$ and radius 0.25. The data are taken such that the exact solution in polar coordinates (r, θ) is

$$u_r = \begin{cases} c_{in}r & \text{in } \Omega^{in} \\ (r - \frac{b^2}{r})c_{ex} + \frac{b^2}{r} & \text{in } \Omega^{ex} \end{cases}, \quad u_\theta = 0, \quad p = \begin{cases} -2c_{in}\lambda_{in} & \text{in } \Omega^{in} \\ -2c_{ex}\lambda_{ex} & \text{in } \Omega^{ex} \end{cases},$$

310 where the constants c_i depend on the Lamé coefficients λ_i, μ_i . The latter are computed from the Poisson coefficients $\nu_{in} = 0.49, \nu_{ex} = 0.25$ and from the Young modulus $E_{in} = E_{ex} = 1$. A Dirichlet boundary condition is imposed on $\partial\Omega$ and treated weakly in the formulation, by means of Nitsche's method. We take the stabilisation parameter on the interface $\lambda = 100$.

315 We show in Table 6 the errors computed on a sequence of uniformly refined meshes, as well as the convergence rates computed from the successive errors. We numerically obtain optimal orders, that is $O(h)$ for the L^2 -norm of the pressure and for the energy norm of the velocity, and $O(h^2)$ for the L^2 -norm of the velocity.

The second test-case deals with a two-phase flow in a rectangular geometry. Let $\Omega = (0, 0.1) \times (-t, t)$ separated in an upper and a lower domain Ω^{in} and Ω^{ex} by a linear interface Γ of equation $y = \zeta t$, see Figure 5 (a). We take $t = 0.01\text{m}$ and $\zeta = -0.2$. The viscosities of the fluids are $\mu_{in} = 100 \text{ Pa}\cdot\text{s}$ and $\mu_{ex} = 10 \text{ Pa}\cdot\text{s}$. At the inflow Γ_{in} we impose the velocity:

$$\mathbf{u} \cdot \mathbf{t} = 0, \quad \mathbf{u} \cdot \mathbf{n} = \begin{cases} 1 - e^{-\gamma(y+t)} & \text{if } y \leq 0 \\ 1 - e^{\gamma(y-t)} & \text{if } y > 0 \end{cases}, \quad \gamma = 2000,$$

320 whereas at the outflow Γ_{out} , a homogeneous Neumann condition is imposed. On the remaining part of the boundary Γ_D , a homogeneous Dirichlet condition is

N	$\ p - p_h\ _{0,\Omega}$	order	$\ \mathbf{u} - \mathbf{u}_h\ _h$	order	$\ \mathbf{u} - \mathbf{u}_h\ _{0,\Omega}$	order
64	0.900	-	5.270	-	3.11×10^{-1}	-
256	0.440	1.028	3.090	0.773	1.05×10^{-1}	1.565
1 024	0.830	1.298	1.490	1.049	2.50×10^{-2}	2.070
4 096	0.373	1.150	0.735	1.021	5.97×10^{-3}	2.063
16 384	0.177	1.077	0.364	1.014	1.45×10^{-3}	2.046

Table 6: Errors and convergence rates for Stokes flow with exact solution

satisfied and $\mathbf{g} = \mathbf{0}$ on the interface Γ . From a physical point of view, this flow is similar to a rectangular Poiseuille flow. Ideally, a flat inflow profile should be imposed; however, in order to avoid discontinuity of the velocity at the corners, we have chosen a quasi-flat profile, see also Figure 6 (a).

It is then easy to obtain the analytical solution when the flow is developed, that is when $u_1 = u_1(y)$ and $u_2 = 0$, by imposing a gradient of pressure $a = \frac{\partial p}{\partial x}$. Thanks to the transmission conditions, we obtain the analytical solution:

$$u_1^{in}(y) = \frac{a}{2\mu_{in}}(t - y)((k - 1)t - y), \quad u_1^{ex}(y) = \frac{a}{2\mu_{ex}}(t + y)(y - (k + 1)t)$$

where $k = \frac{(\mu_{ex} - \mu_{in})(1 - \zeta^2)}{\mu_{in}(1 + \zeta) + \mu_{ex}(1 - \zeta)}$.

In Figure 5 (b), one can see a comparison between the analytical and numerical results at $x = 0.05\text{m}$, where the flow is totally developed. Note that the two profiles of velocity are in very good agreement.

We show in Figure 7 the computed pressure. As expected, in the region where the flow is totally developed the pressure is linear with respect to x and independent of y . We observe a peak at the entrant upper corner, which is due to the high values of the viscosity μ_{in} and of the shear rate $\frac{\partial u_1^{in}}{\partial y}$ near this corner; together they imply a high value of the shear stress. As one can observe in Figure 6 (b), a larger pressure is needed in order to move the more viscous fluid of Ω^{in} ; we see again that the two pressures become linear and equal to each other, starting at $x = 0.02\text{m}$.

Figure 8, showing the two components of the velocity, confirms that the flow is developed quite quickly. As expected, the highest values of the velocity are attained in the less viscous fluid. Figure 6 (a) shows the velocity profiles at different values of x in the transition zone; one can see again the acceleration of the less viscous fluid and the deceleration of the more viscous one.

Although the employed mesh is not aligned with the interface, these tests show that we obtain the expected physical behaviour, without any numerical oscillations at the interface.

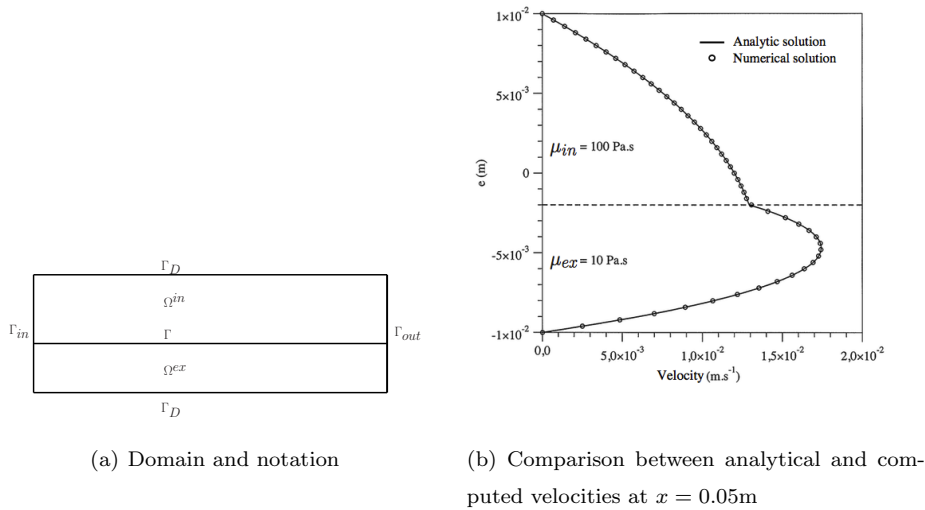


Figure 5: Two-phase Poiseuille flow

7. Concluding remarks

In this paper, we have introduced two NXFEM methods with nonconforming elements and we have studied their robustness. We have shown that both proposed methods exhibit the same behaviour as the conforming one, with respect to the position of the interface and to the diffusion coefficients. It is important to note that we have taken into account both aspects simultaneously, which leads to an open question regarding the interpolation error of the inter-

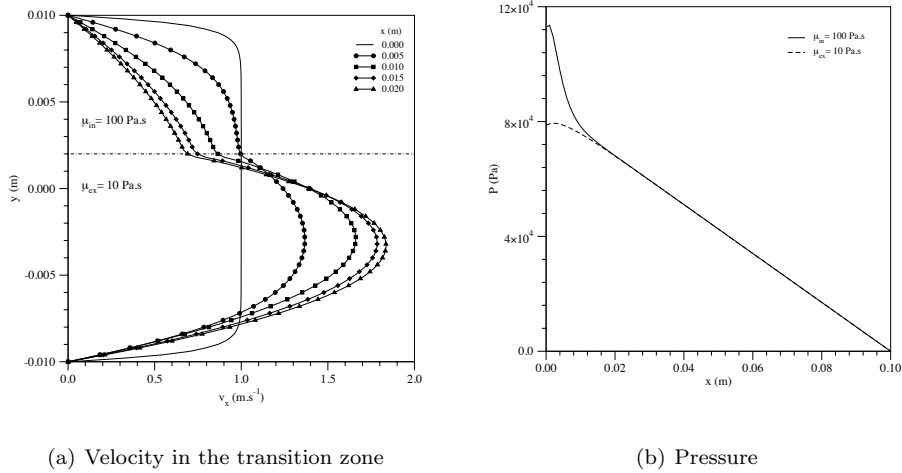


Figure 6: Profiles of the computed solution



Figure 7: Computed pressure

face term $\lambda_T^{1/2} \|[v - I_h v]\|_{0,\Gamma_T}$. This question arises independently of the chosen finite elements: conforming, nonconforming or completely discontinuous.

355 We recall (see Remark 1) that if the ratio μ^{in}/μ^{ex} is uniformly bounded from below and from above, then the previous interpolation error becomes robust with respect to the position of the interface, for all the methods discussed here.

We have implemented both variants with nonconforming elements (10) and (17). From a numerical point of view, the obtained results are very similar; they

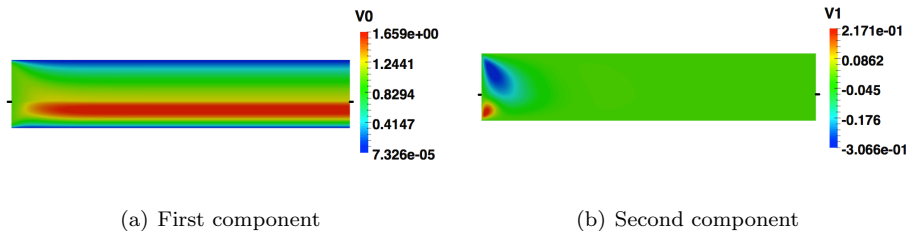


Figure 8: Computed velocity

360 also compare well with those given by the conforming NXFEM method.

From an implementation point of view, the nonconforming method with modified basis functions (17) needs the integration of exactly the same terms as the conforming NXFEM method. So, once the new basis functions on the cut cells are implemented, one could re-use the software developed for the conforming approximation. In our opinion, this is an important advantage of this formulation. Note that for the nonconforming formulation (10) one has to integrate additional terms on the cut edges, which need additional geometrical information.

From a theoretical point of view, the advantage of (10), and implicitly of its dG variant (18), consists in the standard proof of their robustness. Indeed, this can be obtained by means of Strang's lemma. Note that the analysis of the consistency error is completely classical, since it involves only whole edges, whereas for the interpolation error, we can use the Crouzeix-Raviart operator. Thus, we only have to analyse the interpolation error in the additional term in the norm, which is due to the stabilisation. We have been able to establish a robust estimate by using a precise trace inequality on a cut segment. We have then deduced the robustness of the second method (17) by passing to the limit in the dG method.

380 However, we couldn't manage to prove the uniform robustness of (17) by following the standard approach based on Strang's lemma, as for the first formulation (10). More precisely, the constant of the interpolation error in the

H^1 -semi-norm on the quadrilateral part of a cut cell may blow up when the interface is close to the edge. In the Appendix, we explain the reason of this behaviour and how this could eventually be improved.

385 8. Appendix: Interpolation error for the modified Crouzeix-Raviart elements

Contrarily to the stabilised nonconforming method, we have to use a different interpolation operator, denoted by $\tilde{I}_h = (\tilde{I}_h^{in}, \tilde{I}_h^{ex})$, on the modified space \tilde{V}_h of the formulation (17). On the non-cut cells, \tilde{I}_h coincides with the classical
390 Crouzeix-Raviart operator whereas on the cut cells, it is associated to the new basis functions.

We focus on the H^1 -interpolation error on the cut cells, which is the main issue. In view of applying the Bramble-Hilbert lemma, we first need to estimate the norms of the modified basis functions on the cut cells.

This can be done in an optimal way with respect to the position of the interface. By using the definition of the basis functions, the passage to the reference element and the relations:

$$\frac{|T^\Delta|}{|T|} = (1 - \alpha)(1 - \beta), \quad \frac{|T^\square|}{|T|} = 1 - (1 - \alpha)(1 - \beta) \simeq \alpha + \beta,$$

395 we have proved the next result.

Proposition 1. *Let any $T \in \mathcal{T}_h^\Gamma$. Then*

$$\begin{aligned} \sum_{k=1}^3 |\varphi_k^\square|_{1,T^\square} &\simeq \frac{1}{\sqrt{\alpha + \beta}}, & \sum_{k=1}^3 |\varphi_k^\Delta|_{1,T^\Delta} &\simeq \frac{\sqrt{(1 - \alpha)(1 - \beta)}}{1 - \alpha\beta}, \\ \sum_{k=1}^3 \|\varphi_k^\square\|_{0,T^\square} &\simeq \sqrt{\alpha + \beta} h_T, & \sum_{k=1}^3 \|\varphi_k^\Delta\|_{0,T^\Delta} &\simeq \sqrt{(1 - \alpha)(1 - \beta)} h_T. \end{aligned}$$

Clearly, the L^2 -bounds are robust; assuming that the triangular part T^Δ is not degenerate, that is it satisfies $\frac{1 - \alpha}{1 - \beta} \simeq c$, we also get that $\sum_{k=1}^3 |\varphi_k^\Delta|_{1,T^\Delta} \simeq c$.

However, the upper bound of $\sum_{k=1}^3 |\varphi_k^\square|_{1,T^\square}$ blows up as $(\alpha + \beta) \rightarrow 0$.

By applying next the Bramble-Hilbert lemma on T^\square and T^Δ and by using
400 Proposition 1, we have proved:

Proposition 2. Let $T \in \mathcal{T}_h^\Gamma$ be cut in $T^{in} \subset \Omega^{in}$ and $T^{ex} \subset \Omega^{ex}$, such that the triangular part T^Δ is not degenerate. Then there exist constants $c_1 > 0$ and $c_2 > 0$ independent of T and Γ_T such that, for any $v \in H^2(T^i)$, $i = in, ex$:

$$|v - \tilde{I}_T^i v|_{1,T^i} \leq c_1 h_T \left(\sum_{k=1}^3 |\varphi_k^j|_{1,T^i} \right) |E^i v|_{2,T},$$

$$\|v - \tilde{I}_T^i v\|_{0,T^i} \leq c_2 h_T^2 |E^i v|_{2,T}$$

where $j = \square$ if $T^i = T^\square$ and $j = \Delta$ if $T^i = T^\Delta$.

405 Thus, the L^2 -estimates as well as the H^1 -estimate on the triangular part are robust. In order to get a robust H^1 -estimate on the quadrilateral part too, the constant c_1 should compensate the singular behaviour of the basis functions (which cannot be improved). To obtain a constant c_1 independent of the position of the interface, we have applied the Sobolev embedding theorem
 410 on the quadrilateral part of a cut cell: we have bounded the \mathcal{C}^0 -norm on \hat{T}^\square by the \mathcal{C}^0 -norm (and hence, the H^2 -one) on the whole reference triangle \hat{T} . This approach is certainly non-optimal and should be improved in order to get $c_1 \simeq \sqrt{\alpha + \beta}$, leading to a robust H^1 -estimate and finally, to the uniform robustness of the method.

415 References

- [1] C. Annavarapu, M. Hautefeuille, J. Dolbow, A robust Nitsche's formulation for interface problems, *Comput. Methods Appl. Mech. Engrg.* 44 (2012) 225–228.
- [2] N. Barrau, R. Becker, E. Dubach, R. Luce, A robust variant of NXFEM
 420 for the interface problem, *C. R. Acad. Sci. Paris* 350 (2012) 789–792.
- [3] P. Bastian, C. Engwer, An unfitted finite element method using discontinuous Galerkin, *Int. J. Numer. Meth. Engrg.* 79 (2009) 1557–1576.
- [4] R. Becker, E. Burman, P. Hansbo, A Nitsche extended finite element method for incompressible elasticity with discontinuous modulus of elasticity, *Comput. Methods Appl. Mech. Eng.* 41-44 (2009) 3352–3360.
 425

- [5] R. Becker, D. Capatina, J. Joie, Connections between discontinuous Galerkin and nonconforming finite element methods for the Stokes equations, *Numer. Methods Partial Differential Eqs.* 28 (2012) 1013–1041.
- [6] E. Burman, M. Fernandez, An unfitted Nitsche method for incompressible fluid-structure interaction using overlapping meshes, *Comput. Methods in Appl. Mech. Eng.* 279 (2014) 497–514.
- [7] E. Burman, P. Hansbo, A unified stabilized method for Stokes’ and Darcy’s equations, *J. Comput. Appl. Math.* 198 (2007) 35–51.
- [8] E. Burman, P. Hansbo, Fictitious domain methods using cut elements: III. A stabilized Nitsche method for Stokes problem, *Math. Model. Numer. Anal.* 48 (2014) 859–874.
- [9] M. Crouzeix, P.A. Raviart, Conforming and nonconforming finite element methods for solving the stationary Stokes equations, *R.A.I.R.O.* 7 (1973) 33–75.
- [10] D. Di Pietro, A. Ern, *Mathematical Aspects of Discontinuous Galerkin Methods*, SMAI Mathématiques et Applications, Springer, 2012.
- [11] D. Di Pietro, A. Ern, J.L. Guermond, Discontinuous Galerkin methods for anisotropic semidefinite diffusion with advection, *SIAM J. Numer. Anal.* 46 (2008) 805–831.
- [12] H. El-Otmany, *Approximation par la méthode NXFEM des problèmes d’interface et d’interphase en mécanique des fluides*, Ph.D. thesis, University of Pau, Pau (France), 2015.
- [13] A. Hansbo, P. Hansbo, An unfitted finite element method based on Nitsche’s method for elliptic interface problems, *Comput. Methods Appl. Mech. Engng.* 191 (2002) 5537–5552.
- [14] P. Hansbo, M. Larson, S. Zahedi, A cut finite element method for a Stokes interface problem, *Applied Numer. Math.* 85 (2014) 90–114.

- [15] A. Massing, M. Larson, A. Logg, M. Rognes, A stabilized Nitsche fictitious domain method for the Stokes problem, *J. Sci. Comput.* 61 (2014) 604–628.
- 455 [16] A. Massing, M. Larson, A. Logg, M. Rognes, A Nitsche-based cut finite element method for a fluid - structure interaction problem, *CAMCoS* 10 (2015) 97–120.
- [17] R. Massjung, An unfitted discontinuous Galerkin method applied to elliptic interface problems, *SIAM J. Numer. Anal.* 50 (2012) 3134–3162.
- 460 [18] J. Nitsche, Über ein variationsprinzip zur Lösung von Dirichlet-Problemen bei Verwendung von Teilräumen, die keinen Randbedingungen unterworfen sind, *Abh. Math. Sem. Univ. Hamburg* 36 (1971) 9–15.